Hindawi
Mathematical Problems in Engineering
Volume 2019, Article ID 4924306, 15 pages
https://doi.org/10.1155/2019/4924306

*Research Article*

# Wave-Based Method for Free Vibration Analysis of Orthotropic Cylindrical Shells with Arbitrary Boundary Conditions

**Fuzhen Pang**,[1] **Ruidong Huo**,[1] **Haichao Li**,[1] **Cong Gao**,[1] **Xuhong Miao**,[1,2] **and Yi Ren**[1]

[1]*College of Shipbuilding Engineering, Harbin Engineering University, Harbin 150001, China*
[2]*Naval Research Academy, Beijing 100161, China*

Correspondence should be addressed to Haichao Li; lihaichao@hrbeu.edu.cn and Xuhong Miao; miaoxuhong@aliyun.com

Received 31 May 2019; Revised 19 August 2019; Accepted 4 September 2019; Published 22 September 2019

Academic Editor: Stylianos Georgantzinos



The wave-based method (WBM) is a feasible method which investigates the free vibration characteristics of orthotropic cylindrical shells under general boundary conditions. Based on Reissner–Naghid's shell theory, the governing motion equation is established, and the displacement variables are transformed into wave functions formed to satisfy the governing equations. On the basis of the kinematic relationship between the force resultant and displacement vector, the overall matrix of the shell is established. Comparison studies of this paper with the solutions in the literatures were carried out to validate the accuracy of the present method. Furthermore, by analyzing some numerical examples, the free vibration characteristics of orthogonal anisotropic cylindrical shells under classical boundary conditions, elastic boundary conditions, and their combinations are studied. Also, the effects of the material parameter and geometric constant on the natural frequencies for the orthotropic circular cylindrical shell under general boundary conditions are discussed. The conclusions obtained can be used as data reference for future calculation methods.

## 1. Introduction

Orthotropic materials have good material properties, and they are very popular in the engineering application field. As a common engineering geometry, cylindrical shell structure has certain applications in petroleum equipment, coal development, and marine equipment. Because of the development of research in recent years, the free vibration analysis of the orthotropic circular cylindrical shells under general boundary conditions has gradually deepened. With the development of cylindrical shell theory in recent decades, more and more theories are put forward and developed. At present, the main shell theory related to free vibration of cylindrical shell mainly includes three types, namely, classical shell theory [1–4], first-order shear deformation shell theory [5–8], and high-order shear deformation shell theory [9–11].

Over the decades, many researchers have put in a lot of time and effort on the vibration analysis of the orthotropic circular cylindrical shells and obtained many excellent research results. Chen et al. [12] analyzed the free vibration characteristics of the fluid-filled FG orthotropic cylindrical shells, and the boundary condition was set as simply supported. The 3D anisotropic elasticity fundamental equations were used to state equations and some numerical examples are presented. Ding et al. [13] extended the nonhomogeneous orthotropic elastic solution for the axisymmetric plane strain cylindrical shell dynamic problems, and the orthogonal expansion technique was adopted to derive the time variable and the solutions were obtained. Najafov et al. [14] conducted the Galerkin method to investigate the vibration and stability characteristics of the FG orthotropic cylindrical shells on elastic foundations. Sofiyev and Kuruoglu [15] proposed the vibration and buckling of FG orthotropic cylindrical shells in the same way. The Donnell shell theory and Galerkin method were adopted to derive the governing equation. Mallon et al. [16] proposed the coupled shaker-structure model to study the dynamic stable problem of the harmonically base-excited thin orthotropic cylindrical shell. The numerical observations were qualitatively confirmed by comparing the results with the experimental solutions. Prado et al. [17] presented the nonlinear vibrations and dynamic instability problem for the orthotropic circular

cylindrical shell under simply supported boundary conditions. Donnell's shell theory and Galerkin method were used to establish the differential equations of the shell. Lakis and Selmane [18] conducted the thin shell theory, fluid theory, and the hybrid FEM to study the influence of large amplitude vibration of orthotropic, circumferentially nonuniform cylindrical shells. Ahmed [19] analyzed the isotropic and orthotropic cylindrical shell with variable circumferentially thickness and complex curvature radius by Flugge's shell theory. The transfer-matrix method and the Longberg integral method were proposed in the establishment of the motion control equation. Liu et al. [20] proposed the S-DQFEM to investigate the free vibration problem of the orthotropic circular cylindrical shells under classical boundary conditions, and the Donnell–Mushtari shell theory was adopted. Furthermore, the natural frequencies of the closed-form are obtained by the method of variable separation. Sofiyev and Aksogan [21] extended the Galerkin method to investigate the free vibration characteristics of the nonhomogeneous orthotropic thin cylindrical shells with geometric nonlinearity. Fang et al. [22] investigated the vibration characteristics of nanosized piezoelectric double-shell structures under simply supported boundary condition by the Goldenveizer–Novozhilov shell theory, thin plate theory, and electroelastic surface theory. Zhu et al. [23] studied the surface energy effect on the nonlinear free vibration behavior of orthotropic piezoelectric cylindrical nanoshells by the classical shell theory. Also, for the shell and composite structures, some reported literatures have been discussed. Ghassabi et al. [24] presented the solution strategy based on the state vector technique to study the vibroacoustic performance of carbon nanotube- (CNT-) reinforced composite doubly curved thick shells by three-dimensional theory. Talebitooti et al. [25] conducted the nondominated sorting genetic algorithm to optimize sound transmission loss of the laminated composite cylindrical shell by FSDST. Ghassabi et al. [26] investigated the vibroacoustic performance of the doubly curved thick shell by the three-dimensional sound propagation approach and state space solution. Talebitooti et al. [27] analyzed the acoustic characteristics of the doubly curved composite shell with full simply supported by the third-order shear deformation theory (TSDT). Talebitooti and Zarastvand [28] investigated the acoustic transmission of the infinitely long doubly curved shell based on HSDT. Talebitooti et al. [29] discussed the effect of compressing porous material on sound transmission loss of the multilayered cylindrical shell subjected to porous core and air-gap insulation in the presence of external flow based on the three-dimensional elasticity theory. Talebitooti and Zarastvand [30] investigated the wave propagation on infinite doubly curved laminated composite shell which is used in aerospace structures. Talebitooti et al. [31] analyzed the acoustic behavior of laminated composite infinitely long doubly curved shallow shells which is the acoustic behavior of laminated composite infinitely long doubly curved shallow shells. Talebitooti et al. [32] analyzed the acoustic behavior of the laminated composite cylindrical shell which is excited by an oblique plane sound wave by the third-order shear deformation theory.

For the wave-based method, it is an unfamiliar semi-analytical method to investigate the dynamic characteristics of the engineering structure in some applications such as cylindrical shell structure [33–35], coupled structure [36–40], coupled vibroacoustic problem [41], composite structure [42–45], and so on.

## 2. Theoretical Formulations

*2.1. Description of the Shell Model.* The model of circular cylindrical shell is described in Figure 1. The circular cylindrical shell is composed of homogeneous and isotropic materials. $h$ represents the cross section of the uniform circular cylindrical shell with thickness. $L$ represents the length of the circular cylindrical shell. The model is described by curvilinear coordinate system ($x$, $\theta$, and $z$), in which $x$ and $\theta$ denote the axial and circumferential directions of the shell, respectively. The displacements in the direction of $x$, $\theta$, and $z$ of the middle surface are denoted as $u$, $v$, and $w$, respectively. For the elastic boundary conditions, there are three pair translational restrained springs ($K_u$, $K_v$, and $K_w$) and one pair rotational restrained spring ($K_\theta$) are set at two ends to simulate the arbitrary elastic boundary conditions.

*2.2. Kinematic Relations and Stress Resultants.* According to Reissner–Naghid's shell theory [46], the relationship between the strain resultant $\boldsymbol{\varepsilon}^0 = \{\varepsilon^0_{xx}, \varepsilon^0_{\theta\theta}, \varepsilon^0_{x\theta}\}^{\mathrm{T}}$ and curvature change resultant $\boldsymbol{\chi}^0 = \{\chi^0_{xx}, \chi^0_{\theta\theta}, \chi^0_{x\theta}\}^{\mathrm{T}}$ in the middle surface of the shell is shown as follows:

$$\begin{aligned}
\varepsilon^0_{xx} &= \frac{\partial u}{\partial x},\\
\varepsilon^0_{\theta\theta} &= \frac{\partial v}{R\,\partial\theta} + \frac{w}{R},\\
\varepsilon^0_{x\theta} &= \frac{\partial v}{\partial x} + \frac{\partial u}{R\,\partial\theta},\\
\chi^0_{xx} &= -\frac{\partial^2 w}{\partial x^2},\\
\chi^0_{\theta\theta} &= \frac{\partial v}{R^2\partial\theta} - \frac{\partial^2 w}{R^2\partial\theta^2},\\
\chi^0_{x\theta} &= \frac{\partial v}{R\,\partial x} - 2\frac{\partial^2 w}{R\,\partial x\,\partial\theta}.
\end{aligned} \tag{1}$$

Furthermore, the strains of arbitrary point in the shell are given as follows:

$$\begin{aligned}
\varepsilon_{xx} &= \varepsilon^0_{xx} + z\chi^0_{xx},\\
\varepsilon_{\theta\theta} &= \varepsilon^0_{\theta\theta} + z\chi^0_{\theta\theta},\\
\varepsilon_{x\theta} &= \varepsilon^0_{x\theta} + z\chi^0_{x\theta}.
\end{aligned} \tag{2}$$

Also, the stress-strain relationships of the orthotropic shell are obtained by Hooke's law [47–49]:

$$\begin{Bmatrix} \sigma_{xx} \\ \sigma_{\theta\theta} \\ \tau_{x\theta} \end{Bmatrix} = \begin{bmatrix} Q_{11} & Q_{12} & 0 \\ Q_{21} & Q_{22} & 0 \\ 0 & 0 & Q_{66} \end{bmatrix} \begin{Bmatrix} \varepsilon_{xx} \\ \varepsilon_{\theta\theta} \\ \varepsilon_{x\theta} \end{Bmatrix}, \tag{3}$$

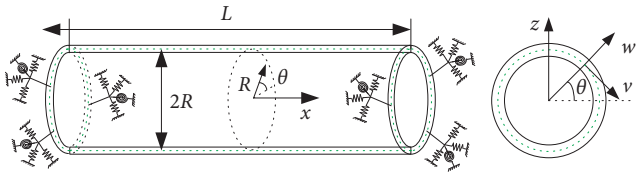


Figure 1: The schematic diagram of the orthotropic circular cylindrical shell.

where $Q_{ij}\,(i, j = 1, 2, 6)$ are the transform coefficients which are defined as follows:

$$\begin{aligned} Q_{11} &= \frac{E_1}{1-\mu_{12}\mu_{21}}, \\ Q_{12} = Q_{21} &= \frac{\mu_{12}E_2}{1-\mu_{12}\mu_{21}}, \\ Q_{22} &= \frac{E_2}{1-\mu_{12}\mu_{21}}, \\ Q_{66} &= G_{12}, \end{aligned} \tag{4}$$

where $E_1$ and $E_2$ are the Young's modulus, $\mu_{12}$ and $\mu_{21}$ are the Poisson's ratios, and $G_{12}$ is the shear modulus. The relationship between $\mu_{12}$ and $\mu_{21}$ is determined as $\mu_{21}E_1 = \mu_{12}E_2$. For the isotropic cylindrical shell, the relationship is defined as $E_1 = E_2$ and $G_{12} = E_1/(2 + 2\mu_{12})$. To obtain the force vector and bending moment resultant of the orthotropic shell, the relationship between the force resultant, bending moment, and strain vector is given as follows:

$$\begin{aligned} \begin{Bmatrix} N_x \\ N_\theta \\ N_{x\theta} \end{Bmatrix} &= \int_z \begin{Bmatrix} \sigma_{xx} \\ \sigma_{\theta\theta} \\ \tau_{x\theta} \end{Bmatrix} dz, \\ \begin{Bmatrix} M_x \\ M_\theta \\ M_{x\theta} \end{Bmatrix} &= \int_z \begin{Bmatrix} \sigma_{xx} \\ \sigma_{\theta\theta} \\ \tau_{x\theta} \end{Bmatrix} z\, dz. \end{aligned} \tag{5}$$

So, the expression for the resultant forces and moments is as follows:

$$\begin{bmatrix} N_x \\ N_\theta \\ N_{x\theta} \\ M_x \\ M_\theta \\ M_{x\theta} \end{bmatrix} = \begin{bmatrix} A_{11} & A_{12} & 0 & 0 & 0 & 0 \\ A_{21} & A_{22} & 0 & 0 & 0 & 0 \\ 0 & 0 & A_{66} & 0 & 0 & 0 \\ 0 & 0 & 0 & D_{11} & D_{12} & 0 \\ 0 & 0 & 0 & D_{21} & D_{22} & 0 \\ 0 & 0 & 0 & 0 & 0 & D_{66} \end{bmatrix} \begin{bmatrix} \varepsilon^0_{xx} \\ \varepsilon^0_{\theta\theta} \\ \varepsilon^0_{x\theta} \\ \chi^0_{xx} \\ \chi^0_{\theta\theta} \\ \chi^0_{x\theta} \end{bmatrix}, \tag{6}$$

where $A_{ij}$ and $D_{ij}\,(i, j = 1, 2, 6)$ are the coefficients and are defined as follows:

$$\begin{aligned} A_{ij} &= Q_{ij}h, \\ D_{ij} &= \frac{h^3}{12}Q_{ij}. \end{aligned} \tag{7}$$

*2.3. Governing Equations.* Based on Reissner–Naghid's theory, the governing equation of the orthotropic cylindrical shell in terms of the force resultant, moment vector, and displacement variables are given as follows [50–52]:

$$\begin{aligned} \frac{\partial N_x}{\partial x} + \frac{1}{R}\frac{\partial N_{x\theta}}{\partial \theta} &= \rho h \frac{\partial^2 u}{\partial t^2}, \\ \frac{\partial N_{x\theta}}{\partial x} + \frac{1}{R}\frac{\partial N_\theta}{\partial \theta} + \frac{1}{R}\frac{\partial M_{x\theta}}{\partial x} + \frac{1}{R^2}\frac{\partial M_\theta}{\partial \theta} &= \rho h \frac{\partial^2 v}{\partial t^2}, \\ \frac{\partial^2 M}{\partial x^2} + \frac{2}{R}\frac{\partial^2 M_{x\theta}}{\partial x\,\partial \theta} + \frac{1}{R^2}\frac{\partial^2 M_\theta}{\partial \theta^2} - \frac{N_\theta}{R} &= \rho h \frac{\partial^2 w}{\partial t^2}, \end{aligned} \tag{8}$$

where $\rho$ is the destiny of the orthotropic circular cylindrical shell. Submitting the expression of force and moment resultant into equation (8), the governing equation of the orthotropic cylindrical shell is given in the matrix form as follows:

$$\begin{bmatrix} T_{11} & T_{12} & T_{13} \\ T_{21} & T_{22} & T_{23} \\ T_{31} & T_{32} & T_{33} \end{bmatrix} \begin{Bmatrix} u \\ v \\ w \end{Bmatrix} = \rho h \begin{Bmatrix} \dfrac{\partial^2 u}{\partial t^2} \\ \dfrac{\partial^2 v}{\partial t^2} \\ \dfrac{\partial^2 w}{\partial t^2} \end{Bmatrix}, \tag{9}$$

where $T_{ij}\,(i, j = 1, 2, 3)$ are the transform coefficients, and the expression of them are given as follows:

$$\begin{aligned} T_{11} &= A_{11}\frac{\partial^2}{\partial x^2} + \frac{A_{66}}{R^2}\frac{\partial^2}{\partial \theta^2}, \\ T_{12} &= \frac{(A_{12} + A_{66})}{R}\frac{\partial^2}{\partial x\,\partial \theta}, \\ T_{13} &= \frac{A_{12}}{R}\frac{\partial}{\partial x}, \\ T_{21} &= \frac{(A_{66} + A_{21})}{R}\frac{\partial^2}{\partial x\,\partial \theta}, \\ T_{22} &= \left(A_{66} + \frac{D_{66}}{R^2}\right)\frac{\partial^2}{\partial x^2} + \left(\frac{A_{22}}{R^2} + \frac{D_{22}}{R^4}\right)\frac{\partial^2}{\partial \theta^2}, \\ T_{23} &= -\frac{D_{22}}{R^4}\frac{\partial^3}{\partial \theta^3} - \left(\frac{D_{21} + 2D_{66}}{R^2}\right)\frac{\partial^3}{\partial x^2 \partial \theta} + \frac{A_{22}}{R^2}\frac{\partial}{\partial \theta}, \\ T_{31} &= -\frac{A_{21}}{R}\frac{\partial}{\partial x}, \\ T_{32} &= \frac{D_{22}}{R^4}\frac{\partial^3}{\partial \theta^3} + \frac{D_{12} + 2D_{66}}{R^2}\frac{\partial^3}{\partial x^2 \partial \theta} - \frac{A_{22}}{R^2}\frac{\partial}{\partial \theta}, \\ T_{33} &= -D_{11}\frac{\partial^4}{\partial x^4} - \frac{D_{22}}{R^4}\frac{\partial^4}{\partial \theta^4} - \frac{(D_{12} + D_{21} + 4D_{66})}{R^2} \\ &\quad \cdot \frac{\partial^4}{\partial x^2 \partial \theta^2} - \frac{A_{22}}{R^2}. \end{aligned} \tag{10}$$

*2.4. Implementation of the WBM.* Using the WBM to analyze the free vibration characteristics of the orthotropic cylindrical shell under general boundary conditions, the displacement variables should be transformed into the wave functions form as follows [33]:

$$\begin{aligned} u(x,\theta,t) &= U_0 e^{jk_n x}\cos(n\theta)e^{-j\omega t},\\ v(x,\theta,t) &= V_0 e^{jk_n x}\sin(n\theta)e^{-j\omega t},\\ w(x,\theta,t) &= W_0 e^{jk_n x}\cos(n\theta)e^{-j\omega t}, \end{aligned} \tag{11}$$

where $U_0$, $V_0$, and $W_0$ are the displacement amplitude variables, $k_n$ is the axial wave number, $t$ is the time variable, $n$ is the circumferential number, and $\omega$ is the circular frequency. So, submitting equation (11) into equation (9), the governing equation of the orthotropic cylindrical shell in the wave function form is obtained as follows:

$$\begin{bmatrix} L_{11} & L_{12} & L_{13}\\ L_{21} & L_{22} & L_{23}\\ L_{31} & L_{32} & L_{33} \end{bmatrix} \begin{Bmatrix} U_0\\ V_0\\ W_0 \end{Bmatrix} = \begin{bmatrix} -\rho h\omega^2 & 0 & 0\\ 0 & \rho h\omega^2 & 0\\ 0 & 0 & \rho h\omega^2 \end{bmatrix} \begin{Bmatrix} U_0\\ V_0\\ W_0 \end{Bmatrix}, \tag{12}$$

where $L_{ij}\,(i, j = 1, 2, 3)$ are the coefficients of equation (12) in the wave functions form, and the expressions are given as follows:

$$\begin{aligned} L_{11} &= -\frac{A_{66}n^2}{R^2} - A_{11}k_n^2,\\ L_{12} &= ink_n\left(\frac{A_{12}+A_{66}}{R}\right),\\ L_{13} &= \frac{ik_nA_{12}}{R},\\ L_{21} &= \frac{ink_n(A_{21}+A_{66})}{R},\\ L_{22} &= A_{66}k_n^2 + \frac{A_{22}n^2}{R^2} + \frac{D_{66}k_n^2}{R^2} + \frac{D_{22}n^2}{R^4},\\ L_{23} &= \frac{(D_{21}+2D_{66})nk_n^2}{R^2} + \frac{nA_{22}}{R^2} + \frac{D_{22}n^3}{R^4},\\ L_{31} &= \frac{ik_nA_{21}}{R},\\ L_{32} &= \frac{(D_{12}+2D_{66})nk_n^2}{R^2} + \frac{nA_{22}}{R^2} + \frac{D_{22}n^3}{R^4},\\ L_{33} &= D_{11}k_n^4 + \frac{(D_{12}+D_{21}+4D_{66})n^2k_n^2}{R^2} + \frac{A_{22}}{R^2} + \frac{D_{22}n^4}{R^4}. \end{aligned} \tag{13}$$

To make sure equation (13) has nontrivial solutions, the determinant of the coefficient matrix in equation (12) should be equal to zero. Also, the eighth-order equation of the axial wave number $k_n$ is obtained as follows:

$$a_8k_n^8 + a_6k_n^6 + a_4k_n^4 + a_2k_n^2 + a_0 = 0, \tag{14}$$

where $a_i\,(i = 0, 2, 4, 6, 8)$ are the coefficients of the eighth-order equation, and the solutions of equation (14) are calculated by Reference [53] as follows:

$$k_n = \pm k_n^1,\ \pm k_n^2,\ \pm k_n^3,\ \pm k_n^4, \tag{15}$$

where $k_n^i\,(i = 1, 2, 3, 4)$ can be in real, imaginary, and combination form. Furthermore, the displacement variables in the wave function forms are converted as follows:

$$\begin{Bmatrix} u(x,\theta,t)\\ v(x,\theta,t)\\ w(x,\theta,t) \end{Bmatrix} = \sum_{n=0}^{\infty}\sum_{i=1}^{8} \begin{Bmatrix} \lambda_{n,i}W_{0,i}e^{jk_n^i x}\cos(n\theta)\\ \kappa_{n,i}W_{0,i}e^{jk_n^i x}\sin(n\theta)\\ W_{0,i}e^{jk_n^i x}\cos(n\theta) \end{Bmatrix} e^{-j\omega t}, \tag{16}$$

where $\lambda_{n,i}$ and $\kappa_{n,i}$ are the wave contribution factors which are expressed as follows:

$$\begin{aligned} \lambda_{n,i} &= \frac{\begin{vmatrix} L_{13} & L_{12}\\ L_{23} & L_{22} \end{vmatrix}}{\begin{vmatrix} L_{12} & L_{11}\\ L_{22} & L_{21} \end{vmatrix}_{n,i}},\\ \kappa_{n,i} &= \frac{\begin{vmatrix} L_{11} & L_{13}\\ L_{21} & L_{23} \end{vmatrix}}{\begin{vmatrix} L_{12} & L_{11}\\ L_{22} & L_{21} \end{vmatrix}_{n,i}}. \end{aligned} \tag{17}$$

Particularly, the expressions for displacement variables are transformed as follows:

$$\begin{Bmatrix} u(x,\theta,t)\\ v(x,\theta,t)\\ w(x,\theta,t) \end{Bmatrix} = \sum_{n=0}^{\infty}\sum_{i=1}^{8} \begin{Bmatrix} \overline{u}(x)W_{n,i}\cos(n\theta)\\ \overline{v}(x)W_{n,i}\sin(n\theta)\\ \overline{w}(x)W_{n,i}\cos(n\theta) \end{Bmatrix} e^{-j\omega t}, \tag{18}$$

where

$$\begin{aligned} \overline{u}(x) &= \lambda_{n,i}e^{jk_n^i x},\\ \overline{v}(x) &= \kappa_{n,i}e^{jk_n^i x},\\ \overline{w}(x) &= e^{jk_n^i x}. \end{aligned} \tag{19}$$

On the basis of the relationship between the displacement variables and force and moment resultants, the detailed expression of the force resultant and moment vector is shown as follows:

$$\begin{Bmatrix} N_x(x,\theta,t)\\ M_x(x,\theta,t)\\ N_{x\theta}(x,\theta,t)\\ Q_x(x,\theta,t) \end{Bmatrix} = \sum_{n=0}^{\infty}\sum_{i=1}^{8} \begin{Bmatrix} \overline{N_x}(x)W_{n,i}\cos(n\theta)\\ \overline{M_x}(x)W_{n,i}\cos(n\theta)\\ \overline{N_{x\theta}}(x)W_{n,i}\sin(n\theta)\\ \overline{Q_x}(x)W_{n,i}\cos(n\theta) \end{Bmatrix} e^{-j\omega t}, \tag{20}$$

where

$$\begin{aligned}
\overline{N_x}(x) &= \left(ik_n^i A_{11}\lambda_{n,i} + \frac{nA_{12}}{R}\kappa_{n,i} + \frac{A_{12}}{R}\right)e^{jk_n^i x},\\
\overline{M_x}(x) &= \left(\frac{nD_{12}}{R^2}\kappa_{n,i} + \frac{D_{12}n^2}{R^2} + D_{11}\left(k_n^i\right)^2\right)e^{jk_n^i x},\\
\overline{N_{x\theta}}(x) &= \left(-\frac{nA_{66}}{R}\lambda_{n,i} + ik_n^i A_{66}\kappa_{n,i}\right)e^{ik_n^i x},\\
\overline{Q_x}(x) &= \left(ink_n^i\frac{D_{12}+D_{66}}{R^2}\kappa_{n,i} + iD_{11}\left(k_n^i\right)^3\right.\\
&\quad \left. + \frac{in^2k_n^i\left(D_{12}+2D_{66}\right)}{R^2}\right)e^{jk_{n,i}x}.
\end{aligned} \tag{21}$$

For the classical boundary conditions, four type of boundary conditions are considered which are widely used in some engineering applications, as follows [54–56]:

Free (F):

$$N_x = N_{x\theta} + \frac{M_{x\theta}}{R} = Q_x + \frac{\partial M_{x\theta}}{\partial\theta} = M_x = 0. \tag{22}$$

Clamped (C):

$$u = v = w = \frac{\partial w}{\partial x} = 0. \tag{23}$$

Simply supported (SS):

$$u = v = w = M_x = 0. \tag{24}$$

Shear diaphragm (SD):

$$N_x = v = w = M_x = 0. \tag{25}$$

For the elastic boundary conditions, the relationship between the force, displacement, and elastic restrained stiffness is discussed. When the elastic restrained stiffness is in the axial direction, the boundary relationship is given as follows:

$$K_u u(x,\theta,t) \pm N_x(x,\theta,t) = 0, \tag{26}$$

where $K_u$ is the stiffness constant, and the symbol $\pm$ means the elastic restrained spring at the boundary edge $x = L$ and $x = 0$. Also, for the circumferential displacement, the normal displacement, and the transverse normal rotations of the $\theta$ and $x$ axis, the symbol $\pm$ has the same meaning for the elastic boundary conditions. For the other elastic restrained states, the boundary relationships can refer to Reference [57]. Related to the introduction of the elastic and classical boundary conditions, the final equation of the orthotropic cylindrical shell is given as follows:

$$[\mathbf{K}]\{\mathbf{W}\} = \{\mathbf{F}\}, \tag{27}$$

where $\mathbf{K}$ is the overall matrix, $\mathbf{F}$ is the external force resultant, and $\mathbf{W} = \{\mathbf{W}_1; \mathbf{W}_2\}$ is the wave contribution factor vector. $\mathbf{W}_1$ and $\mathbf{W}_2$ are the wave contribution factor vectors which are related to the boundary conditions at the two ends. The overall matrix $\mathbf{K}$ is shown as follows:

$$[\mathbf{K}] = \begin{bmatrix} [\mathbf{D}_1(0)] & \\ [\mathbf{B}_1(L)] & [\mathbf{B}_2(0)] \\ & [\mathbf{D}_2(0)] \end{bmatrix}, \tag{28}$$

where $\mathbf{D}_1$ and $\mathbf{D}_2$ are the boundary matrixes which depend on the boundary conditions and $\mathbf{B}_1$ and $\mathbf{B}_2$ are the segment matrixes which are given as follows:

$$\mathbf{B}_{1,2}(x) = \pm\begin{bmatrix} \boldsymbol{\delta}(x) \\ \mathbf{f}(x) \end{bmatrix}, \tag{29}$$

where $\boldsymbol{\delta}(x)$ and $\mathbf{f}(x)$ are the displacement and force matrix of the orthotropic shell and are expressed as follows:

$$\begin{aligned}
\boldsymbol{\delta}(x) &= \begin{bmatrix} \overline{u_1}(x) & \overline{u_2}(x) & \cdots & \overline{u_8}(x) \\ \overline{v_1}(x) & \overline{v_2}(x) & \cdots & \overline{v_8}(x) \\ \overline{w_1}(x) & \overline{w_2}(x) & \cdots & \overline{w_8}(x) \\ \dfrac{\partial\overline{w_1}(x)}{\partial x} & \dfrac{\partial\overline{w_2}(x)}{\partial x} & \cdots & \dfrac{\partial\overline{w_8}(x)}{\partial x} \end{bmatrix},\\
\mathbf{f}(x) &= \begin{bmatrix} \overline{N_{x,1}}(x) & \overline{N_{x,2}}(x) & \cdots & \overline{N_{x,8}}(x) \\ \overline{M_{x,1}}(x) & \overline{M_{x,2}}(x) & \cdots & \overline{M_{x,8}}(x) \\ \overline{N_{x\theta,1}}(x) & \overline{N_{x\theta,2}}(x) & \cdots & \overline{N_{x\theta,8}}(x) \\ \overline{Q_{x,1}}(x) & \overline{Q_{x,2}}(x) & \cdots & \overline{Q_{x,8}}(x) \end{bmatrix}.
\end{aligned} \tag{30}$$

When analyzing the free vibration characteristics of the orthotropic cylindrical shell under general boundary conditions, the external force vector $\mathbf{F}$ should be vanished. For each circumferential number $n$, searching the zero position of the overall matrix $\mathbf{K}$, a series of values are calculated. When the sign occurs, the natural frequencies of the cylindrical shell are obtained.

The dichotomy method is a mathematical idea that uses flat partitions and infinite approximations. It is an effective algorithm for avoiding complex calculations and approximations of analytic one-dimensional functions. In this paper, the dichotomy method is adopted to get the natural frequencies of the cylindrical shell, and some numerical examples are established.

## 3. Numerical Examples and Discussion

In this part, some numerical examples are presented to investigate the free vibration characteristics of the orthotropic cylindrical shell under general boundary conditions (i.e., classical, elastic, and combinations). Some numerical examples are extended to verify the correctness of the results by the presented method. Furthermore, the effects of the material parameter and geometric constants on the free

vibration characteristics of the orthotropic circular cylindrical shell are studied.

*3.1. Orthotropic Cylindrical Shell with Classical and Elastic Boundary Conditions.* First, the comparison of the natural frequencies for the homogeneous cylindrical shell under clamped-clamped boundary condition is presented. The results by the present method are compared with the solutions by Ref. [58] in Table 1. The geometric parameters and material constants are defined as follows: $L = 511.2$ mm, $R = 216.2$ mm, $h = 1.5$ mm, $E = 1.83 \times 10^{11}$ N/m$^2$, $\mu = 0.3$, and $\rho = 7492$ kg/m$^3$. The range of the circumferential mode number $n$ and longitudinal wave number $m$ is set as 2–6 and 1–3. It can be seen that the results of the two methods are in good agreement, and the maximum error is 5.79% which appears with $n = 3$ and $m = 1$. Next, this paper discusses the free vibration characteristics of the orthotropic cylindrical shell under classical boundary conditions. To verify the correctness of the results by the presented method, the natural frequencies of the orthotropic cylindrical shell under several classical boundary conditions are compared with the solutions in the reported literature by Zhao et al. [59]. There are three pair classical boundary conditions which are set as SS-SS, SD-SD, and C-C. The material parameters are given as follows: $E_1 = 120$ GPa, $E_2 = 10$ GPa, $G_{12} = 5.5$ GPa, $\mu_{12} = 0.27$, and $\rho = 1700$ kg/m$^3$. The geometric constants are set as follows: $L = 5$ m, $h = 0.01$ m, and $R = 1$ m. In Table 2, the natural frequencies of the first two longitudinal modes for the first six circumferential numbers are calculated. By comparing the MRRM in the reference literature and the results by the presented method, we can discover that the errors are small. It is obvious that the free vibration characteristics for the orthotropic circular cylindrical shell under classical boundary conditions calculated by the presented method are correct. From Table 1, we can find that for each circumferential number and longitudinal mode, the minimum natural frequency is associated with the boundary condition SD-SD and the maximum natural frequency is related to the boundary condition C-C. It can be concluded that the classical boundary conditions have a significant effect on the free vibration characteristics for the orthotropic circular cylindrical shell.

Next, the free vibration characteristics of the orthotropic circular cylindrical shell under classical combination boundary conditions are concerned. The material parameters and geometric constants are equal to the numerical example in Table 2. For the classical combination boundary conditions, there are two type boundary conditions, C-F and SS-F, which are considered, and the results by the presented method are compared with the solutions by the MRRM method [59]. From Table 2, the errors between the two numerical methods are small, and the maximum error is 0.95%. So, it can be concluded that the free vibration characteristics which are investigated by the presented method are right. From the two numerical examples in Tables 2 and 3, the free vibration characteristics for orthotropic circular cylindrical shell under classical boundary conditions and their combinations are discussed. Figure 2 shows some modes of orthotropic cylindrical shells under C-C boundary conditions. The purpose is to further study the free vibration characteristics of orthotropic cylindrical shells under classical boundary conditions.

Next, the free vibration characteristics of the orthotropic circular cylindrical shell under elastic boundary conditions and their combinations are concerned. In this paper, there are three type elastic-restrained situations which are considered as follows:

First-elastic boundary condition (EBC_1): the axial displacement is under elastic restrained and others are fixed ($u \neq 0$, $v = w = \partial w/\partial x = 0$), and the elastic stiffness value is set as $K_u = 10^9$.

Second-elastic boundary condition (EBC_2): the circumferential displacement is under elastic restrained and others are fixed ($v \neq 0$, $u = w = \partial w/\partial x = 0$), and the elastic stiffness value is set as $K_v = 10^9$.

Third-elastic boundary condition (EBC_3): the radial displacement is under elastic restrained and others are fixed ($w \neq 0$, $u = v = \partial w/\partial x = 0$), and the elastic stiffness value is set as $K_w = K_\theta = 10^7$.

In Table 4, there are six type elastic boundary conditions and their combinations (i.e., EBC1-EBC1, EBC2-EBC2, EBC3-EBC3, EBC1-EBC3, EBC2-EBC3, and EBC1-EBC2) are concerned. The first five circumferential numbers (i.e., $n = 1$–5) and the first four longitudinal modes (i.e., $m = 1$–4), natural frequencies for the orthotropic circular cylindrical shells under several elastic boundary conditions, are calculated. The material parameters and geometric constants are the same as the numerical example in previous discussion. For various elastic boundary conditions, the natural frequencies are relatively stable within a range and have a small variation range for various circumferential numbers and longitudinal modes. Also, some mode shapes of the orthotropic circular cylindrical shell with EBC1-EBC1 are shown in the Figure 3.

*3.2. Effect of the Material and Geometric Parameters on the Natural Frequencies.* In addition, the effect of the material parameter and geometric constants on the natural frequencies for the orthotropic circular cylindrical shell under several boundary conditions (i.e., C-C, S-F, EBC_1-EBC_2, and EBC_3-EBC_3) is discussed.

First, the effect of the modulus ratio $E_1/E_2$ for the orthotropic circular cylindrical shell under various boundary conditions is discussed. The material parameter and geometric constants are similar to the numerical example in the previous study. The changing rule of the modulus ratio $E_1/E_2$ is from 1 to 12, the natural frequencies for the first two circumferential number (i.e., $n = 1$ and 2) and the first four longitudinal mode (i.e., $m = 1$–4) under various boundary conditions are calculated in Table 5. For analyzing the effect of the modulus ratio $E_1/E_2$, the changing rule of the natural frequencies under various boundary conditions is shown in the Figure 4 ($n = 1$). It is obvious that with the changing of the modulus ratio $E_1/E_2$, the natural frequencies are generally growing for various longitudinal modes under various boundary conditions. Also, for the boundary condition S-F,

Table 1: Comparison of the natural frequencies for the homogeneous cylindrical shell under clamped-clamped boundary conditions.

| $n$ | $m=1$ | | | $m=2$ | | | $m=3$ | | |
|---|---|---|---|---|---|---|---|---|---|
| | Present | Reference [58] | Error (%) | Present | Reference [58] | Error (%) | Present | Reference [58] | Error (%) |
| 2 | 1281.90 | 1299 | 1.32 | 2593.52 | 2660 | 2.50 | 4245.89 | 4364 | 2.71 |
| 3 | 2110.36 | 2240 | 5.79 | 2555.82 | 2574 | 0.71 | 3389.93 | 3483 | 2.67 |
| 4 | 3830.74 | 3872 | 1.07 | 4082.66 | 4043 | −0.98 | 4473.30 | 4417 | −1.27 |
| 5 | 6240.10 | 6262 | 0.35 | 6383.64 | 6491 | 1.65 | 6645.01 | 6728 | 1.23 |
| 6 | 9087.86 | 9125 | 0.41 | 9129.98 | 9276 | 1.57 | 9259.20 | 9540 | 2.94 |

Table 2: Comparison of the natural frequencies for the orthotropic circular cylindrical shell under classical boundary conditions.

| Boundary conditions | Method | $n=1$ | $n=2$ | $n=3$ $m=1$ | $n=4$ | $n=5$ | $n=1$ | $n=2$ | $n=3$ $m=2$ | $n=4$ | $n=5$ |
|---|---|---|---|---|---|---|---|---|---|---|---|
| C-C | Present | 122.7511 | 76.4642 | 52.8701 | 41.4866 | 39.4239 | 225.6351 | 146.3284 | 103.4431 | 79.3989 | 67.0333 |
| | Reference [59] | 122.75 | 76.464 | 52.869 | 41.486 | 39.423 | 225.63 | 146.33 | 103.44 | 79.398 | 67.033 |
| | Error (%) | 0.00 | 0.00 | 0.00 | 0.00 | 0.00 | 0.00 | 0.00 | 0.00 | 0.00 | 0.00 |
| SS-SS | Present | 122.5910 | 76.1294 | 52.4352 | 41.0422 | 39.0609 | 225.2716 | 145.6195 | 102.4194 | 78.1700 | 65.7589 |
| | Reference [59] | 122.59 | 76.129 | 52.435 | 41.042 | 39.061 | 225.27 | 145.62 | 102.42 | 78.17 | 65.759 |
| | Error (%) | 0.00 | 0.00 | 0.00 | 0.00 | 0.00 | 0.00 | 0.00 | 0.00 | 0.00 | 0.00 |
| SD-SD | Present | 117.9855 | 66.1809 | 40.8206 | 30.8837 | 32.3243 | 225.2414 | 144.7009 | 99.8179 | 74.0717 | 61.0129 |
| | Reference [59] | 117.99 | 66.181 | 40.821 | 30.884 | 32.324 | 225.24 | 144.7 | 99.818 | 74.072 | 61.01 |
| | Error (%) | 0.00 | 0.00 | 0.00 | 0.00 | 0.00 | 0.00 | 0.00 | 0.00 | 0.00 | 0.00 |

Table 3: Comparison of the natural frequencies for the orthotropic circular cylindrical shell under combination classical boundary conditions.

| Boundary conditions | Method | $n=1$ | $n=2$ | $n=3$ $m=1$ | $n=4$ | $n=5$ | $n=1$ | $n=2$ | $n=3$ $m=2$ | $n=4$ | $n=5$ |
|---|---|---|---|---|---|---|---|---|---|---|---|
| C-F | Present | 57.2692 | 29.4248 | 18.4766 | 19.1837 | 27.1424 | 166.7386 | 96.3363 | 62.8738 | 46.8067 | 42.1131 |
| | Reference [59] | 57.272 | 29.445 | 18.566 | 19.365 | 27.376 | 166.74 | 96.347 | 62.922 | 46.952 | 42.414 |
| | Error (%) | 0.00 | −0.07 | −0.48 | −0.94 | −0.86 | 0.00 | −0.01 | −0.08 | −0.31 | −0.71 |
| SS-F | Present | 57.2303 | 29.3770 | 18.4436 | 19.1688 | 27.1366 | 166.6339 | 96.0876 | 62.5356 | 46.4639 | 41.8393 |
| | Reference [59] | 57.233 | 29.397 | 18.532 | 19.35 | 27.369 | 166.64 | 96.098 | 62.584 | 46.609 | 42.137 |
| | Error (%) | 0.00 | −0.07 | −0.48 | −0.95 | −0.86 | 0.00 | −0.01 | −0.08 | −0.31 | −0.71 |

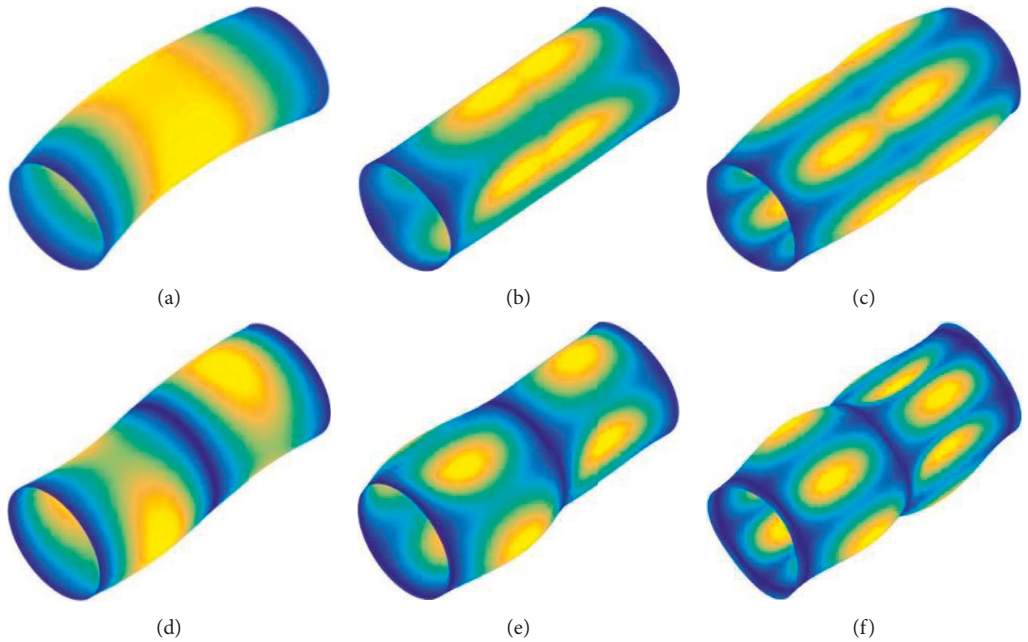

Figure 2: The mode shapes of the orthotropic circular cylindrical shell under C-C boundary condition. (a) $n=1$, $m=1$, (b) $n=2$, $m=1$, (c) $n=3$, $m=1$, (d) $n=1$, $m=2$, (e) $n=2$, $m=2$, and (f) $n=3$, $m=2$.

Table 4: The natural frequencies for the orthotropic circular cylindrical shell under elastic boundary conditions and their combinations.

| $n$ | $m$ | Boundary conditions | | | | | |
|---|---|---|---|---|---|---|---|
| | | EBC1-EBC1 | EBC2-EBC2 | EBC3-EBC3 | EBC1-EBC3 | EBC2-EBC3 | EBC1-EBC2 |
| 1 | 1 | 121.211 | 122.513 | 122.741 | 121.859 | 122.627 | 120.6801 |
| | 2 | 225.634 | 225.269 | 225.618 | 225.626 | 225.444 | 223.8509 |
| | 3 | 295.019 | 294.726 | 294.998 | 295.008 | 294.862 | 293.584 |
| | 4 | 332.953 | 332.765 | 332.924 | 332.939 | 332.845 | 332.059 |
| 2 | 1 | 72.788 | 76.340 | 76.442 | 74.491 | 76.391 | 73.89489 |
| | 2 | 146.075 | 146.074 | 146.289 | 146.194 | 146.182 | 145.0127 |
| | 3 | 208.553 | 208.389 | 208.619 | 208.581 | 208.504 | 207.2762 |
| | 4 | 255.979 | 255.727 | 255.920 | 255.950 | 255.823 | 254.7795 |
| 3 | 1 | 48.121 | 52.807 | 52.844 | 50.435 | 52.826 | 50.16391 |
| | 2 | 102.408 | 103.281 | 103.387 | 102.929 | 103.334 | 102.2252 |
| | 3 | 154.456 | 154.656 | 154.785 | 154.613 | 154.720 | 153.7046 |
| | 4 | 199.167 | 199.040 | 199.161 | 199.166 | 199.100 | 198.2201 |
| 4 | 1 | 36.929 | 41.458 | 41.463 | 39.174 | 41.460 | 39.06892 |
| | 2 | 77.503 | 79.304 | 79.336 | 78.464 | 79.320 | 78.08885 |
| | 3 | 120.575 | 121.249 | 121.294 | 120.930 | 121.271 | 120.3684 |
| | 4 | 160.463 | 160.585 | 160.623 | 160.546 | 160.604 | 159.9009 |
| 5 | 1 | 36.110 | 39.413 | 39.407 | 37.717 | 39.410 | 37.6851 |
| | 2 | 64.670 | 66.982 | 66.973 | 65.868 | 66.978 | 65.69338 |
| | 3 | 99.855 | 100.974 | 100.959 | 100.409 | 100.967 | 100.0973 |
| | 4 | 134.854 | 135.270 | 135.241 | 135.051 | 135.256 | 134.6571 |

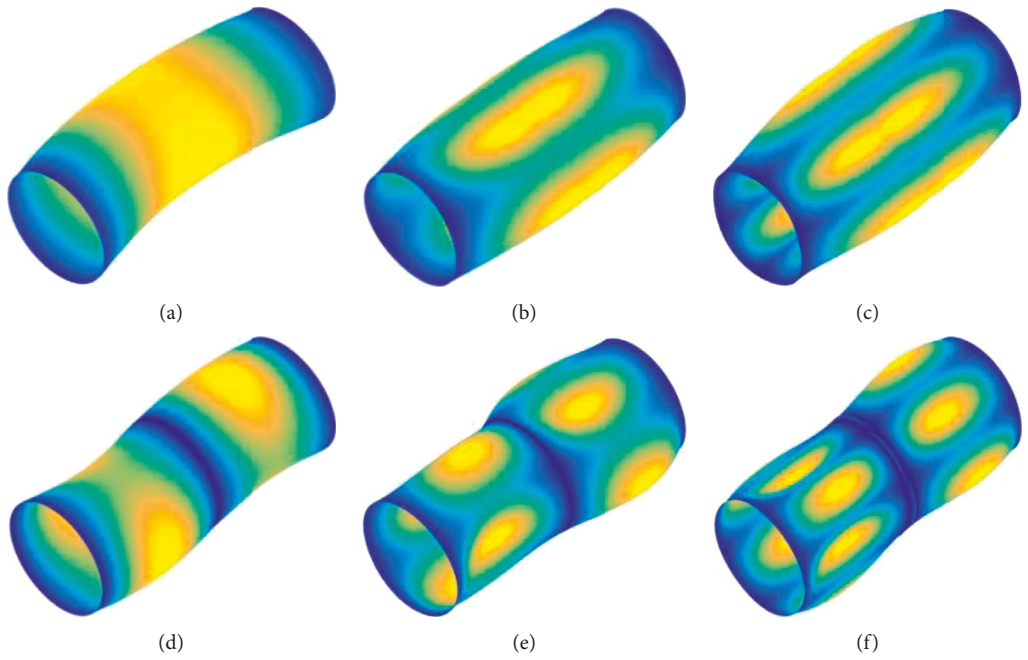


Figure 3: The mode shapes of the orthotropic circular cylindrical shell under EBC1-EBC1 boundary condition. (a) $n = 1$, $m = 1$, (b) $n = 2$, $m = 1$, (c) $n = 3$, $m = 1$, (d) $n = 1$, $m = 2$, (e) $n = 2$, $m = 2$, and (f) $n = 3$, $m = 2$.

the change range of the natural frequencies is more obvious for various longitudinal modes. For other boundary conditions, the change range for the first two longitudinal modes (i.e., $m = 1$ and 2) are evident, and for the longitudinal mode $m = 3$, the change range stays in the basic stable range.

Next, the effect of the geometric constants on the natural frequencies for the orthotropic circular cylindrical shell under several boundary conditions is discussed. In this paper, the geometric constants are set as thickness to radius ratio $h/R$ and length to radius ratio $L/R$. For the boundary conditions, geometric and material parameters are same as the numerical example in the previous study for the effect of the modulus ratio $E_1/E_2$. In Table 6, the natural frequencies for the orthotropic circular cylindrical shell with the changing of the thickness to radius ratios $h/R$ are calculated. The changing range of the thickness to radius ratios $h/R$ is set as 0.001 to 0.1. The natural frequencies are generally increased for various circumferential number and longitudinal

Table 5: The natural frequencies of the orthotropic cylindrical shell with various modulus ratios $E_1/E_2$ under several boundary conditions.

| $E_1/E_2$ | $m$ | Boundary conditions | | | | | | | |
|---|---|---|---|---|---|---|---|---|---|
| | | C-C | | SS-F | | EBC1-EBC2 | | EBC3-EBC3 | |
| | | $n=1$ | $n=2$ | $n=1$ | $n=2$ | $n=1$ | $n=2$ | $n=1$ | $n=2$ |
| 1 | 1 | 110.6992 | 55.2536 | 31.2626 | 11.6005 | 108.9950 | 54.0279 | 110.6879 | 55.2403 |
| | 2 | 211.2475 | 120.7196 | 119.1539 | 58.5856 | 209.0331 | 118.8745 | 211.2434 | 120.7013 |
| | 3 | 292.7848 | 188.8046 | 234.6133 | 132.9303 | 291.0075 | 186.7130 | 292.7825 | 188.7881 |
| 3 | 1 | 119.3153 | 68.6970 | 45.3992 | 18.7554 | 117.2422 | 66.4857 | 119.3085 | 68.6849 |
| | 2 | 221.3334 | 136.5006 | 144.2771 | 78.3209 | 219.3547 | 134.6394 | 221.3285 | 136.4841 |
| | 3 | 294.0729 | 201.8201 | 253.0665 | 157.9665 | 292.4997 | 200.0412 | 294.0666 | 201.8009 |
| 5 | 1 | 121.1147 | 72.5290 | 50.8336 | 22.7042 | 118.9951 | 70.0528 | 121.1077 | 72.5153 |
| | 2 | 223.5331 | 140.9972 | 154.0669 | 85.6214 | 221.6405 | 139.3435 | 223.5256 | 140.9765 |
| | 3 | 294.4017 | 205.0738 | 257.5586 | 165.3520 | 292.8816 | 203.4539 | 294.3914 | 205.0469 |
| 8 | 1 | 122.1522 | 74.9725 | 54.7245 | 26.3878 | 120.0403 | 72.3926 | 122.1439 | 74.9555 |
| | 2 | 224.8418 | 144.1636 | 161.5715 | 91.4974 | 223.0119 | 142.7059 | 224.8302 | 144.1353 |
| | 3 | 294.7082 | 207.2162 | 260.3054 | 170.3087 | 293.2317 | 205.7223 | 294.6917 | 207.1771 |
| 10 | 1 | 122.5081 | 75.8520 | 56.1950 | 28.0675 | 120.4149 | 73.2671 | 122.4986 | 75.8326 |
| | 2 | 225.3073 | 145.4115 | 164.5223 | 94.0730 | 223.5032 | 144.0357 | 225.2928 | 145.3778 |
| | 3 | 294.8730 | 208.0499 | 261.2583 | 172.1662 | 293.4169 | 206.6100 | 294.8524 | 208.0026 |
| 12 | 1 | 122.7511 | 76.4642 | 57.2303 | 29.3770 | 120.6801 | 73.8949 | 122.7406 | 76.4423 |
| | 2 | 225.6351 | 146.3284 | 166.6339 | 96.0876 | 223.8509 | 145.0127 | 225.6179 | 146.2894 |
| | 3 | 295.0230 | 208.6741 | 261.9059 | 173.4884 | 293.5837 | 207.2762 | 294.9984 | 208.6188 |

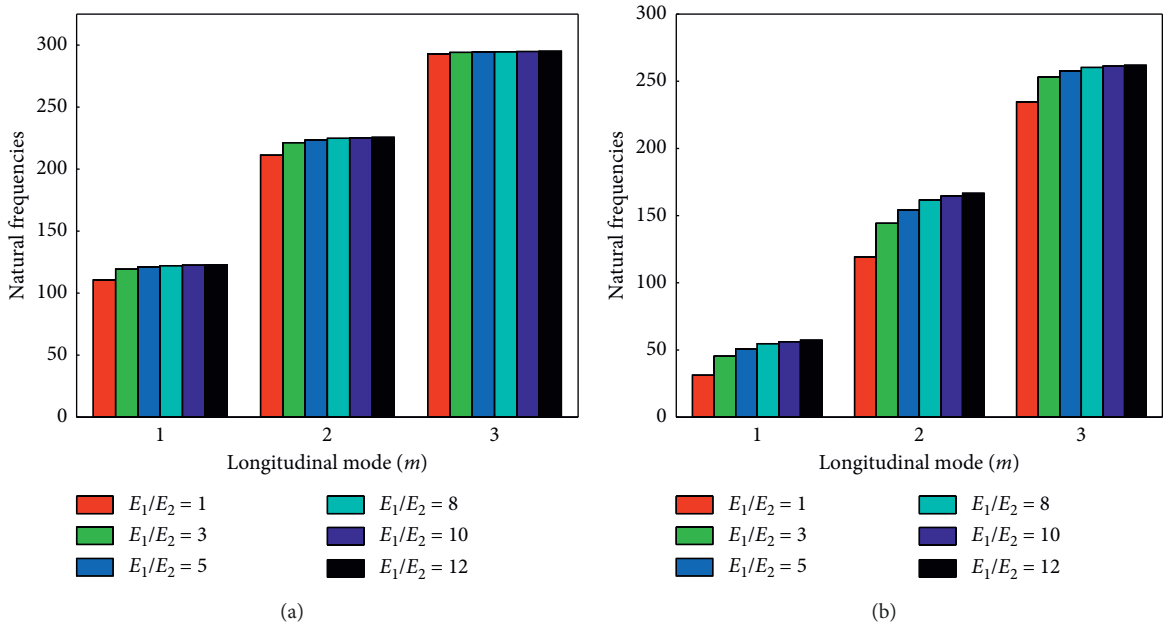


Figure 4: Continued.

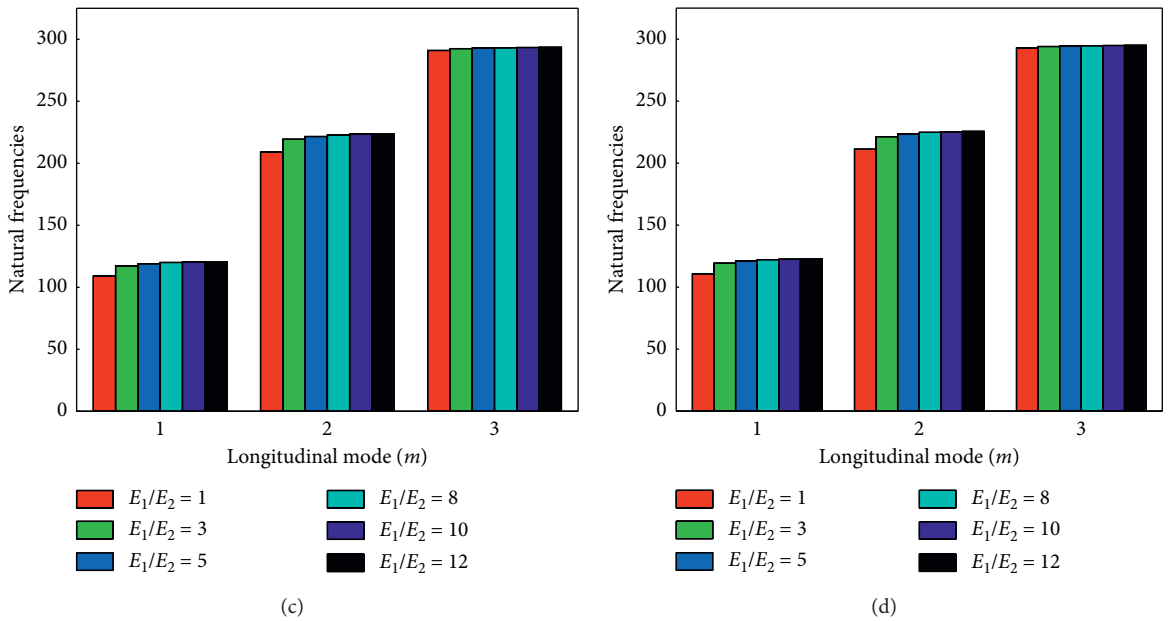


Figure 4: The changing rule of the natural frequencies with various modulus ratios $E_1/E_2$; $n = 1$. (a) C-C, (b) S-F, (c) EBC1-EBC2, and (d) EBC3-EBC3.

Table 6: The natural frequencies of the orthotropic cylindrical shell with various thickness to radius ratios $h/R$ under several boundary conditions.

| $h$ | $m$ | Boundary conditions | | | | | | | |
|---|---|---|---|---|---|---|---|---|---|
| | | C-C | | SS-F | | EBC1-EBC2 | | EBC3-EBC3 | |
| | | $n = 1$ | $n = 2$ | $n = 1$ | $n = 2$ | $n = 1$ | $n = 2$ | $n = 1$ | $n = 2$ |
| 0.001 | 1 | 122.5913 | 76.0481 | 57.2287 | 29.2184 | 122.3553 | 75.6950 | 122.5913 | 76.0480 |
| | 2 | 225.2229 | 145.4536 | 166.6168 | 95.9782 | 225.0297 | 145.2889 | 225.2229 | 145.4535 |
| | 3 | 294.0861 | 207.0796 | 261.7840 | 173.2139 | 293.9218 | 206.8985 | 294.0861 | 207.0795 |
| 0.005 | 1 | 122.6467 | 76.1854 | 57.2295 | 29.2576 | 121.5370 | 74.6696 | 122.6451 | 76.1818 |
| | 2 | 225.3556 | 145.7348 | 166.6211 | 96.0050 | 224.4220 | 144.9893 | 225.3533 | 145.7292 |
| | 3 | 294.3756 | 207.5760 | 261.8143 | 173.2815 | 293.6008 | 206.7692 | 294.3724 | 207.5683 |
| 0.01 | 1 | 122.7511 | 76.4642 | 57.2303 | 29.3770 | 120.6801 | 73.8949 | 122.7406 | 76.4423 |
| | 2 | 225.6351 | 146.3284 | 166.6339 | 96.0876 | 223.8509 | 145.0127 | 225.6179 | 146.2894 |
| | 3 | 295.0230 | 208.6741 | 261.9059 | 173.4884 | 293.5837 | 207.2762 | 294.9984 | 208.6188 |
| 0.05 | 1 | 124.3256 | 81.4447 | 57.2392 | 32.9221 | 117.5104 | 76.1999 | 123.8317 | 80.5904 |
| | 2 | 230.6216 | 157.0350 | 167.0094 | 98.6036 | 224.4088 | 154.2499 | 229.4403 | 154.9489 |
| | 3 | 308.5174 | 230.8005 | 264.5660 | 179.5628 | 303.9226 | 227.8976 | 305.9156 | 226.6462 |
| 0.1 | 1 | 127.4686 | 92.6207 | 57.2553 | 42.0016 | 118.1959 | 87.4795 | 125.6479 | 89.6293 |
| | 2 | 242.0943 | 181.4167 | 168.0745 | 105.8049 | 233.3506 | 178.7213 | 236.1977 | 171.4342 |
| | 3 | 343.1045 | 283.8211 | 271.9447 | 196.1988 | 335.7079 | 280.6610 | 322.5592 | 255.6987 |

modes for boundary condition C-C, SS-F, and ECB_3-ECB_3. Furthermore, the natural frequencies are first decreased and then increased with the growing of the thickness to radius ratios $h/R$ under EBC_1-EBC_2. In order to reflect the law of natural frequency change more intuitively, the changing rule of the natural frequencies with the increase of the thickness to radius ratios $h/R$ under several boundary conditions is shown in Figure 5. Especially, when the thickness to radius ratios $h/R$ are set from 0.05 to 0.1 and related to the longitudinal wave number $m = 3$, the growth rates of the natural frequencies are more obvious than the longitudinal wave number $m = 1$ and 2. Also, for the boundary condition S-F and EBC3-EBC-3, when the longitudinal wave number $m = 1$ and 2, the natural frequencies have a small range of variation and is basically kept within a certain range. In particular, when the boundary condition is set to EBC1-EBC1 and longitudinal wave number $m = 1$, as the thickness to radius ratios $h/R$ increases, the natural frequencies tend to decrease, but the variation is small.

Furthermore, the influence of the length to radius ratios $L/R$ on the natural frequencies for the orthotropic circular cylindrical shell under several boundary conditions is calculated in Table 7. The material constants and geometric properties are the same as the numerical study in previous part, and the changing range of the length to radius ratios $L/R$ are set from 5

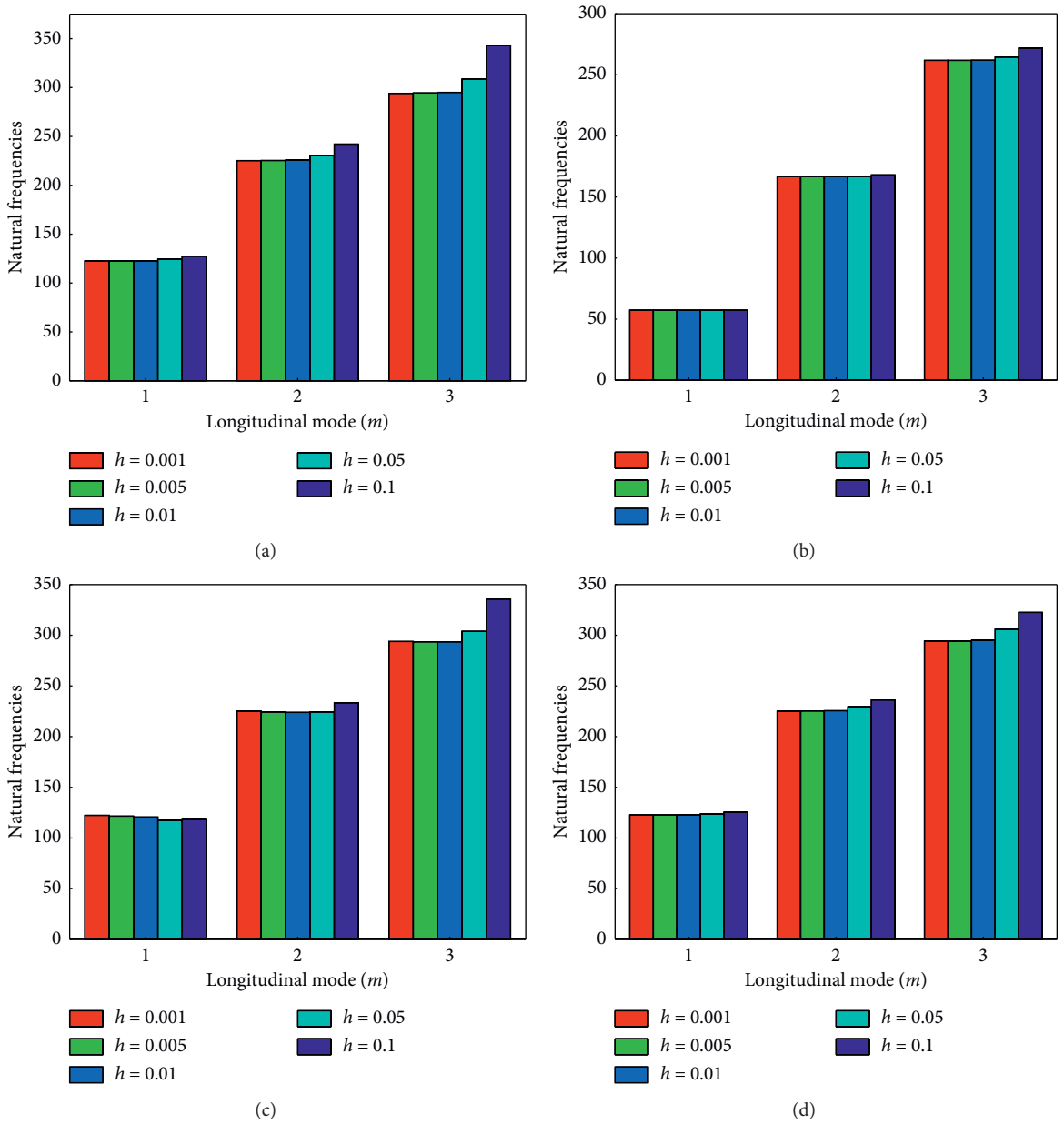


Figure 5: The changing rule of the natural frequencies with various thickness to radius ratios $h/R$; $n = 1$. (a) C-C, (b) S-F, (c) EBC1-EBC2, and (d) EBC3-EBC3.

Table 7: The natural frequencies of the orthotropic cylindrical shell with various length to radius ratios $L/R$ under several boundary conditions.

| $L$ | $m$ | Boundary conditions | | | | | | | |
|---|---|---|---|---|---|---|---|---|---|
| | | C-C | | SS-F | | EBC1-EBC2 | | EBC3-EBC3 | |
| | | $n = 1$ | $n = 2$ | $n = 1$ | $n = 2$ | $n = 1$ | $n = 2$ | $n = 1$ | $n = 2$ |
| 5 | 1 | 122.7511 | 76.4642 | 57.2303 | 29.3770 | 120.6801 | 73.8949 | 122.7406 | 76.4423 |
| | 2 | 225.6351 | 146.3284 | 166.6339 | 96.0876 | 223.8509 | 145.0127 | 225.6179 | 146.2894 |
| | 3 | 295.0230 | 208.6741 | 261.9059 | 173.4884 | 293.5837 | 207.2762 | 294.9984 | 208.6188 |
| 8 | 1 | 76.7055 | 45.4524 | 31.6944 | 14.1556 | 75.2519 | 43.4839 | 76.7009 | 45.4440 |
| | 2 | 148.5210 | 90.2844 | 99.4478 | 53.6849 | 147.5756 | 89.3387 | 148.5141 | 90.2678 |
| | 3 | 214.2263 | 137.1869 | 178.4795 | 107.3297 | 213.0963 | 136.2748 | 214.2159 | 137.1633 |
| 10 | 1 | 60.6792 | 34.7071 | 23.1038 | 9.8312 | 59.4140 | 33.0345 | 60.6761 | 34.7020 |
| | 2 | 118.8628 | 70.3232 | 76.2998 | 39.8337 | 118.1806 | 69.3907 | 118.8582 | 70.3123 |
| | 3 | 176.4915 | 109.1948 | 143.5250 | 82.7372 | 175.6285 | 108.4187 | 176.4847 | 109.1790 |
| 12 | 1 | 49.7780 | 27.4582 | 17.5069 | 7.3573 | 48.6440 | 26.0412 | 49.7758 | 27.4549 |
| | 2 | 98.2672 | 56.7730 | 61.0112 | 30.8062 | 97.7181 | 55.8310 | 98.2638 | 56.7654 |
| | 3 | 148.6260 | 89.5260 | 118.5957 | 65.9236 | 147.9499 | 88.8051 | 148.6211 | 89.5147 |

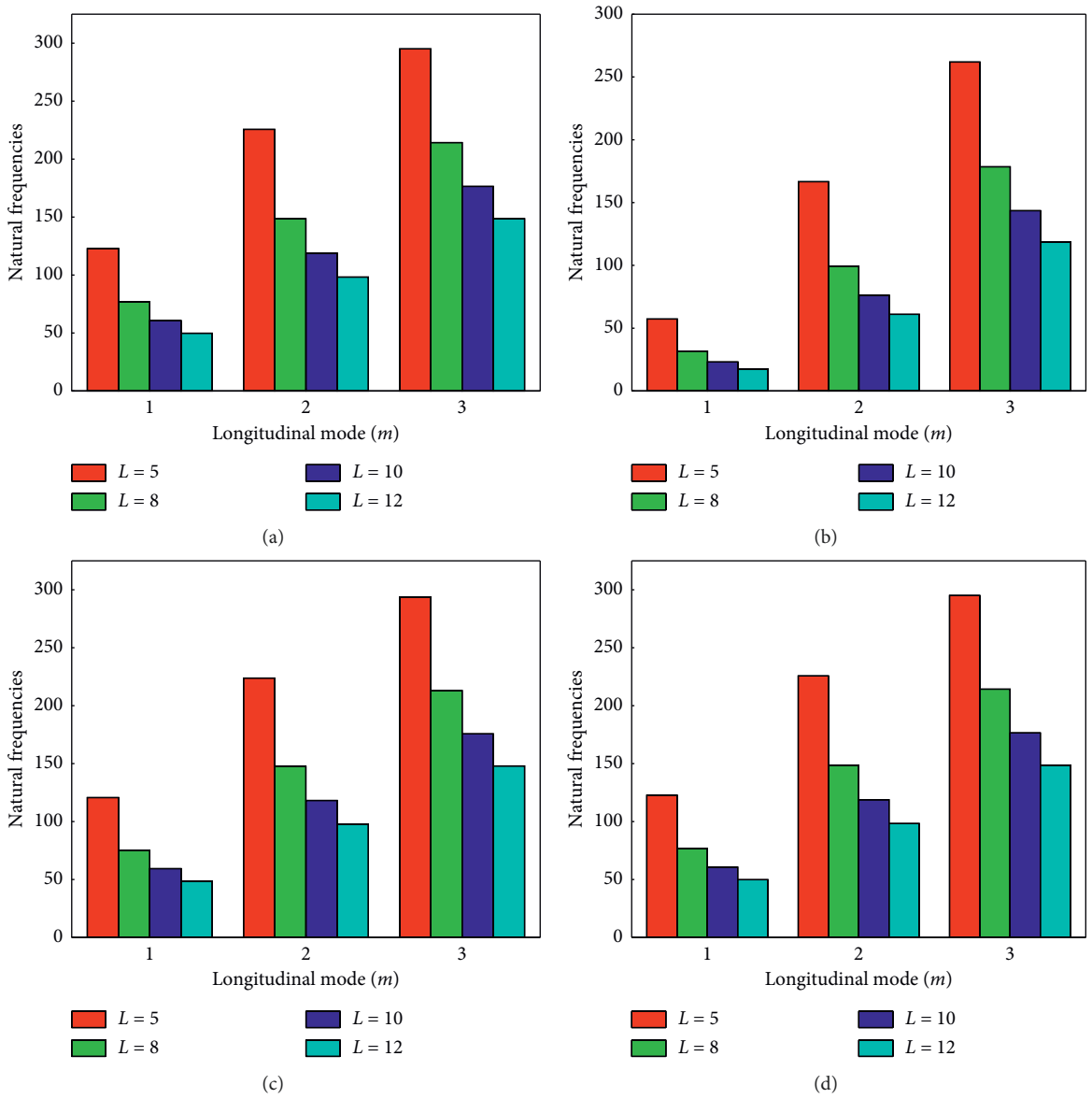


FIGURE 6: The changing rule of the natural frequencies with various length to radius ratios $L/R$; $n = 1$. (a) C-C, (b) S-F, (c) EBC1-EBC2, and (d) EBC3-EBC3.

to 12. In Figure 6, the changing rule of the natural frequencies with respect to the length to radius ratios $L/R$ under various boundary conditions is shown. It can be seen that with the changing of the length to radius ratios $L/R$, the natural frequencies are generally decreased for various boundary conditions related to three longitudinal wave number $m = 1$–$3$, at the same time, and as the length to radius ratios $L/R$ changes, the attenuation effect of the frequency parameters is more obvious. When the length to radius ratios $L/R$ changes from 5 to 8, the decreased attenuations are larger for four type boundary conditions.

## 4. Conclusions

In this paper, a semianalytical method is conducted to investigate the free vibration characteristics of the orthotropic cylindrical shell under general boundary conditions, including the classical boundary conditions, elastic boundary conditions, and their combinations. Reissner–Naghid's shell theory is utilized to obtain the governing motion equations and the displacement variables are transformed into wave function forms to accurate the motion relationship. According to the motion relationship and boundary conditions, the final equation of the orthotropic circular cylindrical shell is established. Then the natural frequencies can be obtained by solving the zero position of the overall matrix determinant based on the dichotomy method. In the numerical examples and discussion parts, the effect of the material parameter and geometric constants on the free vibration characteristics of the orthotropic circular cylindrical shell is studied and some conclusions are obtained.

To verify the correctness of the calculation results by the presented method, some numerical examples are proposed

by comparing with the solutions in the reported literatures. The effect of the material parameter modulus ratio $E_1/E_2$, geometric constants thickness to radius ratio $L/R$, and thickness to radius ratio $h/R$ on the free vibration characteristics of the orthotropic cylindrical shell under several boundary conditions are discussed. For the effect of different parameters, various properties have its one influence impact on the free vibration characteristics of the orthotropic circular cylindrical shell. The changing ranges of the natural frequencies are different for various circumferential number and longitudinal modes under several boundary conditions.

This paper proposed a new numerical method to research the free vibration characteristics of the orthotropic circular cylindrical shell under general boundary conditions, and it provided a theoretical basis for the development of subsequent numerical studies.

## Data Availability

The data used to support the findings of this study are included within the article.

## Conflicts of Interest

The authors declare that there are no conflicts of interest regarding the publication of this paper.

## Acknowledgments

This study was funded by the National Natural Science Foundation of China (nos. 51209052 and 51679053), National key Research and Development Program (2016YFC0303406), Fundamental Research Funds for the Central Universities (HEUCFD1515 and HEUCFM170113), Assembly Advanced Research Fund of China (6140210020105), Naval preresearch project, China Postdoctoral Science Foundation (2014M552661), and Ph.D. Student Research and Innovation Fund of the Fundamental Research Funds for the Central Universities (HEUGIP201801).

## References

[1] S. Akhlaque-E-Rasul and R. Ganesan, "The compressive response of thickness-tapered shallow curved composite plates based on classical shell theory," *Journal of Advanced Materials*, vol. 43, no. 1, pp. 47–65, 2011.

[2] V. Berdichevsky and V. Misyura, "Effect of accuracy loss in classical shell theory," *Journal of Applied Mechanics*, vol. 59, no. 2, pp. S217–S223, 1992.

[3] R. Kienzler, "Eine Erweiterung der klassischen Schalentheorie; der Einflu; von Dickenverzerrungen und Querschnittsverwölbungen," *Ingenieur-Archiv*, vol. 52, no. 5, pp. 311–322, 1982.

[4] K. Wisniewski, "A shell theory with independent rotations for relaxed biot stress and right stretch strain," *Computational Mechanics*, vol. 21, no. 2, pp. 101–122, 1998.

[5] S. Hosseini-Hashemi and M. R. Ilkhani, "Exact solution for free vibrations of spinning nanotube based on nonlocal first order shear deformation shell theory," *Composite Structures*, vol. 157, pp. 1–11, 2016.

[6] I. Kreja, R. Schmidt, and J. N. Reddy, "Finite elements based on a first-order shear deformation moderate rotation shell theory with applications to the analysis of composite structures," *International Journal of Non-linear Mechanics*, vol. 32, no. 6, pp. 1123–1142, 1997.

[7] K. Viswanathan and S. Javed, "Free vibration of anti-symmetric angle-ply cylindrical shell walls using first-order shear deformation theory," *Journal of Vibration & Control*, vol. 22, no. 7, pp. 1757–1768, 2016.

[8] H. Li, F. Pang, H. Chen, and Y. Du, "Vibration analysis of functionally graded porous cylindrical shell with arbitrary boundary restraints by using a semi analytical method," *Composites Part B: Engineering*, vol. 164, pp. 249–264, 2019.

[9] A. M. A. Neves, A. J. M. Ferreira, E. Carrera et al., "Free vibration analysis of functionally graded shells by a higher-order shear deformation theory and radial basis functions collocation, accounting for through-the-thickness deformations," *European Journal of Mechanics—A/Solids*, vol. 37, pp. 24–34, 2013.

[10] E. Viola, F. Tornabene, and N. Fantuzzi, "General higher-order shear deformation theories for the free vibration analysis of completely doubly-curved laminated shells and panels," *Composite Structures*, vol. 95, no. 1, pp. 639–666, 2013.

[11] J. N. Reddy and C. F. Liu, "A higher-order shear deformation theory of laminated elastic shells," *International Journal of Engineering Science*, vol. 23, no. 3, pp. 319–330, 1985.

[12] W. Q. Chen, Z. G. Bian, and H. J. Ding, "Three-dimensional vibration analysis of fluid-filled orthotropic FGM cylindrical shells," *International Journal of Mechanical Sciences*, vol. 46, no. 1, pp. 159–171, 2004.

[13] H. J. Ding, H. M. Wang, and W. Q. Chen, "A solution of a non-homogeneous orthotropic cylindrical shell for axisymmetric plane strain dynamic thermoelastic problems," *Journal of Sound and Vibration*, vol. 263, no. 4, pp. 815–829, 2003.

[14] A. M. Najafov, A. H. Sofiyev, and N. Kuruoglu, "Torsional vibration and stability of functionally graded orthotropic cylindrical shells on elastic foundations," *Meccanica*, vol. 48, no. 4, pp. 829–840, 2013.

[15] A. H. Sofiyev and N. Kuruoglu, "Buckling and vibration of shear deformable functionally graded orthotropic cylindrical shells under external pressures," *Thin-Walled Structures*, vol. 78, pp. 121–130, 2014.

[16] N. J. Mallon, R. H. B. Fey, and H. Nijmeijer, "Dynamic stability of a base-excited thin orthotropic cylindrical shell with top mass: simulations and experiments," *Journal of Sound and Vibration*, vol. 329, no. 15, pp. 3149–3170, 2010.

[17] Z. J. G. N. D. Prado, A. L. D. P. Argenta, F. M. A. Da Silva, and Paulo B. Gonçalves, "The effect of material and geometry on the non-linear vibrations of orthotropic circular cylindrical shells," *International Journal of Non-linear Mechanics*, vol. 66, pp. 75–86, 2014.

[18] A. A. Lakis and A. Selmane, "Hybrid finite element analysis of large amplitude vibration of orthotropic open and closed cylindrical shells subjected to a flowing fluid," *Nuclear Engineering and Design*, vol. 196, no. 1, pp. 1–15, 2000.

[19] M. K. Ahmed, "A new vibration approach of an elastic oval cylindrical shell with varying circumferential thickness," *Journal of Vibration and Control*, vol. 18, no. 1, pp. 117–131, 2012.

[20] B. Liu, Y. F. Xing, M. S. Qatu, and A. J. M. Ferreira, "Exact characteristic equations for free vibrations of thin orthotropic circular cylindrical shells," *Composite Structures*, vol. 94, no. 2, pp. 484–493, 2012.

[21] A. H. Sofiyev and O. Aksogan, "Non-linear free vibration analysis of laminated non-homogeneous orthotropic cylindrical shells," *Proceedings of the Institution of Mechanical Engineers, Part K: Journal of Multi-Body Dynamics*, vol. 217, no. 4, pp. 293–300, 2003.

[22] X.-Q. Fang, C.-S. Zhu, J.-X. Liu, and X.-L. Liu, "Surface energy effect on free vibration of nano-sized piezoelectric double-shell structures," *Physica B: Condensed Matter*, vol. 529, pp. 41–56, 2018.

[23] C.-S. Zhu, X.-Q. Fang, J.-X. Liu, and H.-Y. Li, "Surface energy effect on nonlinear free vibration behavior of orthotropic piezoelectric cylindrical nano-shells," *European Journal of Mechanics—A/Solids*, vol. 66, pp. 423–432, 2017.

[24] M. Ghassabi, M. R. Zarastvand, and R. Talebitooti, "Investigation of state vector computational solution on modeling of wave propagation through functionally graded nanocomposite doubly curved thick structures," *Engineering with Computers*, pp. 1–17, 2019.

[25] R. Talebitooti, H. D. Gohari, and M. R. Zarastvand, "Multi objective optimization of sound transmission across laminated composite cylindrical shell lined with porous core investigating Non-dominated Sorting Genetic Algorithm," *Aerospace Science and Technology*, vol. 69, pp. 269–280, 2017.

[26] M. Ghassabi, R. Talebitooti, and M. R. Zarastvand, "State vector computational technique for three-dimensional acoustic sound propagation through doubly curved thick structure," *Computer Methods in Applied Mechanics and Engineering*, vol. 352, pp. 324–344, 2019.

[27] R. Talebitooti, M. R. Zarastvand, and H. D. Gohari, "The influence of boundaries on sound insulation of the multi-layered aerospace poroelastic composite structure," *Aerospace Science and Technology*, vol. 80, pp. 452–471, 2018.

[28] R. Talebitooti and M. R. Zarastvand, "Vibroacoustic behavior of orthotropic aerospace composite structure in the subsonic flow considering the third order shear deformation theory," *Aerospace Science and Technology*, vol. 75, pp. 227–236, 2018.

[29] R. Talebitooti, A. M. C. Khameneh, M. R. Zarastvand, and M. Kornokar, "Investigation of three-dimensional theory on sound transmission through compressed poroelastic sandwich cylindrical shell in various boundary configurations," *Journal of Sandwich Structures & Materials*, vol. 21, no. 7, pp. 2313–2357, 2019.

[30] R. Talebitooti and M. R. Zarastvand, "The effect of nature of porous material on diffuse field acoustic transmission of the sandwich aerospace composite doubly curved shell," *Aerospace Science and Technology*, vol. 78, pp. 157–170, 2018.

[31] R. Talebitooti, M. Zarastvand, and H. Gohari, "Investigation of power transmission across laminated composite doubly curved shell in the presence of external flow considering shear deformation shallow shell theory," *Journal of Vibration and Control*, vol. 24, no. 19, pp. 4492–4504, 2018.

[32] R. Talebitooti, M. R. Zarastvand, and M. R. Gheibi, "Acoustic transmission through laminated composite cylindrical shell employing third order shear deformation theory in the presence of subsonic flow," *Composite Structures*, vol. 157, pp. 95–110, 2016.

[33] M. Chen, K. Xie, K. Xu, and P. Yu, "Wave based method for free and forced vibration analysis of cylindrical shells with discontinuity in thickness," *Journal of Vibration & Acoustics*, vol. 137, no. 5, 2015.

[34] J. Wei, M Chen, G. Hou, K. Xie, and N. Deng, "Wave based method for free vibration analysis of cylindrical shells with nonuniform stiffener distribution," *Journal of Vibration & Acoustics*, vol. 135, no. 6, Article ID 061011, 2013.

[35] H. Li, F. Pang, X. Miao, and Y. Li, "Jacobi-Ritz method for free vibration analysis of uniform and stepped circular cylindrical shells with arbitrary boundary conditions: a unified formulation," *Computers & Mathematics with Applications*, vol. 77, no. 2, pp. 427–440, 2019.

[36] K. Xie, M. Chen, W. Dong, and W. Li, "A unified semi-analytical method for vibration analysis of shells of revolution stiffened by rings with T cross-section," *Thin-Walled Structures*, vol. 139, pp. 412–431, 2019.

[37] M. Chen, J. Wei, K. Xie, N. Deng, and G. Hou, "Wave based method for free vibration analysis of ring stiffened cylindrical shell with intermediate large frame ribs," *Shock and Vibration*, vol. 20, no. 3, pp. 459–479, 2013.

[38] K. Xie, M. Chen, L. Zhang, and D. Xie, "Wave based method for vibration analysis of elastically coupled annular plate and cylindrical shell structures," *Applied Acoustics*, vol. 123, pp. 107–122, 2017.

[39] H. Li, F. Pang, X. Wang, Y. Du, and H. Chen, "Free vibration analysis of uniform and stepped combined paraboloidal, cylindrical and spherical shells with arbitrary boundary conditions," *International Journal of Mechanical Sciences*, vol. 145, pp. 64–82, 2018.

[40] F. Pang, H. Li, J. Cui, Y. Du, and C. Gao, "Application of flügge thin shell theory to the solution of free vibration behaviors for spherical-cylindrical-spherical shell: a unified formulation," *European Journal of Mechanics—A/Solids*, vol. 74, pp. 381–393, 2019.

[41] W. Desmet, *A Wave Based Prediction Technique for Coupled Vibro-Acoustic Analysis*, Katholieke Universiteit Leuven, Leuven, Belgium, 1998.

[42] H. Li, F. Pang, Y. Li, and C. Gao, "Application of first-order shear deformation theory for the vibration analysis of functionally graded doubly-curved shells of revolution," *Composite Structures*, vol. 212, pp. 22–42, 2019.

[43] H. Li, F. Pang, X. Wang, Y. Du, and H. Chen, "Free vibration analysis for composite laminated doubly-curved shells of revolution by a semi analytical method," *Composite Structures*, vol. 201, pp. 86–111, 2018.

[44] F. Pang, H. Li, H. Chen, and Y. Shan, "Free vibration analysis of combined composite laminated cylindrical and spherical shells with arbitrary boundary conditions," *Mechanics of Advanced Materials and Structures*, pp. 1–18, 2019.

[45] F. Pang, C. Gao, J. Cui, Y. Ren, H. Li, and H. Wang, "A semianalytical approach for free vibration characteristics of functionally graded spherical shell based on first-order shear deformation theory," *Shock and Vibration*, vol. 2019, Article ID 7352901, 18 pages, 2019.

[46] A. W. Leissa, *Vibration of Shells*, Vol. 288, Scientific and Technical Information Office, National Aeronautics and Space Administration, Washington, DC, USA, 1973.

[47] H. Li, F. Pang, Q. Gong, and Y. Teng, "Free vibration analysis of axisymmetric functionally graded doubly-curved shells with un-uniform thickness distribution based on Ritz method," *Composite Structures*, vol. 225, Article ID 111145, 2019.

[48] H. Li, F. Pang, and H. Chen, "A semi-analytical approach to analyze vibration characteristics of uniform and stepped annular-spherical shells with general boundary conditions," *European Journal of Mechanics—A/Solids*, vol. 74, pp. 48–65, 2019.

[49] H. Li, F. Pang, X. Miao, Y. Du, and H. Tian, "A semi-analytical method for vibration analysis of stepped doubly-curved shells of revolution with arbitrary boundary conditions," *Thin-Walled Structures*, vol. 129, pp. 125–144, 2018.

[50] F. Pang, H. Li, X. Wang, X. Miao, and S. Li, "A semi analytical method for the free vibration of doubly-curved shells of revolution," *Computers & Mathematics with Applications*, vol. 75, no. 9, pp. 3249–3268, 2018.

[51] H. Li, F. Pang, X. Miao, S. Gao, and F. Liu, "A semi analytical method for free vibration analysis of composite laminated cylindrical and spherical shells with complex boundary conditions," *Thin-Walled Structures*, vol. 136, pp. 200–220, 2019.

[52] F. Z. Pang et al., "Application of first-order shear deformation theory on vibration analysis of stepped functionally graded paraboloidal shell with general edge constraints," *Materials*, vol. 12, no. 1, 2019.

[53] T. Wah and W. C. L. Hu, "Vibration analysis of stiffened cylinders including inter-ring motion," *The Journal of the Acoustical Society of America*, vol. 43, no. 5, pp. 1005–1016, 1968.

[54] D. Shao, S. Hu, Q. Wang, and F. Pang, "An enhanced reverberation-ray matrix approach for transient response analysis of composite laminated shallow shells with general boundary conditions," *Composite Structures*, vol. 162, pp. 133–155, 2017.

[55] Q. Wang, D. Shi, Q. Liang, and F. Pang, "Free vibrations of composite laminated doubly-curved shells and panels of revolution with general elastic restraints," *Applied Mathematical Modelling*, vol. 46, pp. 227–262, 2017.

[56] H. Li, F. Pang, Y. Ren, X. Miao, and K. Ye, "Free vibration characteristics of functionally graded porous spherical shell with general boundary conditions by using first-order shear deformation theory," *Thin-Walled Structures*, vol. 144, Article ID 106331, 2019.

[57] D. He, D. Shi, Q. Wang, and C. Shuai, "Wave based method (WBM) for free vibration analysis of cross-ply composite laminated cylindrical shells with arbitrary boundaries," *Composite Structures*, vol. 213, pp. 284–298, 2019.

[58] K. K. Viswanathan and P. V. Navaneethakrishnan, "Free vibration study of layered cylindrical shells by collocation with splines," *Journal of Sound and Vibration*, vol. 260, no. 5, pp. 807–827, 2003.

[59] J. Zhao, K. Choe, Y. Zhang, A. Wang, C. Lin, and Q. Wang, "A closed form solution for free vibration of orthotropic circular cylindrical shells with general boundary conditions," *Composites Part B: Engineering*, vol. 159, pp. 447–460, 2019.